# Pattern of scaling violation implied by field theories*

Wu-Ki Tung†
*Enrico Fermi Institute and Department of Physics, University of Chicago, Chicago, Illinois 60637*
(Received 16 July 1975)

The pattern of scaling violation in deep-inelastic scattering implied by renormalizable field theories is studied. A set of model-independent predictions are extracted from a series of model calculations involving both asymptotically free and conventional theories. These are contrasted with the pattern of scaling violation predicted by modified parton models. A procedure for comparing the predictions with experiment is discussed and applied to existing data from the Stanford Linear Accelerator Center. General qualitative agreement is indicated. Crucial tests for the predicted pattern should come from the forthcoming Fermi National Accelerator Laboratory experiments. The possibility of distinguishing the predictions of asymptotically free theories from those of conventional theories by these experiments is found to be untenable due to various uncertainties in the theoretical considerations.

## I. INTRODUCTION

The scaling behavior of the deep-inelastic lepton-hadron scattering structure functions observed at the Stanford Linear Accelerator Center (SLAC) has been the focal point of much theoretical study in the past few years. It suggested the physically appealing interpretation of scattering off pointlike constituents of the hadron target (the parton model).[1] Alternatively, one speaks of canonical light-cone expansion of products of current operators.[1,2] In many ways, these two languages are equivalent.[1] Theoretical attempts to justify either of these simple pictures have, however, met with difficulties.

In particular, within the framework of renormalizable field theories it has been shown that strict Bjorken scaling for the structure functions cannot hold.[3] Violation of scaling invariably arises as a consequence of the renormalization procedure. The rate of this scaling violation can, however, be different for different types of field theories. Thus, the much publicized asymptotically free theories[4] imply a logarithmic scaling violation whereas the conventional-type theories[5] entail a power-law breaking[2] (see Sec. II for precise statements).

In view of the situation, two important questions to bear in mind as the new generation of deep-inelastic lepton-hadron scattering experiments are about to yield results are the following: Will Bjorken scaling persist to these high energies with good accuracy, or will a pattern of scaling violation emerge? In the latter case, will this pattern agree with that implied by field theory? Answers to these questions are crucial toward resolving the long-standing question of whether field theory is relevant for hadron physics.

In fact, as new theoretical techniques for extracting high-energy behavior of the structure functions in field theories advanced to yield more precise predictions (especially for asymptotically free theories), the hope has been raised that these new experiments may even distinguish between the predictions of different types of field theories—thus select out those underlying hadron dynamics. In particular, it appears feasible to distinguish between asymptotically free[4] (hereafter referred to as AF) and the conventional-type[5] (hereafter referred to as CT) theories on account of their different asymptotic behaviors. Thus, since the conception of the theoretically appealing AF theories,[4] several papers have been devoted to the implied scaling violation effects as possible experimental tests of these theories.[6] In order to interpret the comparison of these estimates with experiment in a truly meaningful way, however, it is important to systematically study the similarities and differences between the predictions from CT and AF theories. This has not been done in the literature.

In this paper, we address ourselves to the problems posed in the previous paragraphs. We summarize the existing technique for calculating the structure functions from a set of given initial values at some fixed $q^2 = q_0^2$. From extensive calculations, we extract a fairly specific pattern of scaling violation common to all classes of renormalizable field theories. This is contrasted with other scaling-violation patterns implied by phenomenological models.[8] We compare the predictions with recently available data from SLAC.[9] The comparisons show general agreement but are not necessarily conclusive because of the limited range of existing data. It is pointed out that the soon to be released data from Fermilab should provide crucial tests of the theory. The very preliminary data from the Cornell-Michigan State group[10] are discussed in this context. The prospect for distinguishing the predictions of AF and CT theories within present-day experimental capability is found to be not very promising. This is due to theoretical uncertainties as well as to the

limited $q^2$ range accessible to experiment.

One of the reasons why a systematic study of this kind has not been done previously is the lack of precise knowledge of the "anomalous dimension" parameter $\lambda(n)$ (to be defined in the following section) for CT theories. In this work we overcome this obstacle by adopting a phenomenological parametrization of $\lambda(n)$ consistent with the known general constraints on this function.[11] The pattern of scaling violation extracted from our extensive calculations contains only those aspects which are independent of the parametrization. Therefore, these results are consequences of the general constraints which are known to be reliable.

Since the problems posed in this paper should concern both theorists and experimentalists, the presentation is made to be reasonably self-contained. The main theoretical ideas and calculational techniques are summarized so that experimentalists will be able to compute their own set of curves based on input initial conditions appropriate for their particular experiments.

## II. BASIC FORMALISM

In order to see the basic theoretical ideas clearly, we first consider deep-inelastic scattering through a scalar current $J(z)$. The structure function is just the current correlation function

$$W(x, q^2) = \int d^4q\, e^{iqz}\langle p|J(z)J(0)|p\rangle, \tag{1}$$

where $x = q^2/2M\nu$ and $M\nu = -q\cdot p$. It is a simple property of the Fourier integral that in the Bjorken limit ($q^2\to\infty$, $x$ fixed) the integral on the right-hand side of Eq. (1) is dominated by $\langle p|J(z)J(0)|p\rangle$ near the light cone, i.e., $z^2 = 0$.[1,2] In particular, if $\langle p|J(z)J(0)|p\rangle$ has the simple power behavior

$$\langle p|J(z)J(0)|p\rangle \xrightarrow[z^2\sim 0]{} (z^2)^{-d} c(z\cdot p), \tag{2}$$

then[2] $W(x, q^2) \sim \nu^{d+2}F(x)$ or equivalently,

$$\nu^{-d-2}W(x, q^2) = F(x). \tag{3}$$

Hence one has Bjorken scaling. Unfortunately, renormalizable field theories are incompatible[2,3] with the simple behavior assumed in Eq. (2). Except in the trivial case of free particles, all theories of this kind imply a more complicated singularity structure for the current correlation function near the light cone.[2,3] They invariably lead to violation of strict Bjorken scaling.

The general singularity can be studied by means of the Wilson expansion of the current product,[2]

$$J(z)J(0) = \sum_{n\ \text{even}} z^{\mu_1}z^{\mu_2}\cdots z^{\mu_n} \times \sum_{\alpha} E^n_\alpha(z^2) O^\alpha_{\mu_1\mu_2\cdots\mu_n}(0), \tag{4}$$

where $E^n_\alpha(z^2)$ are $c$-number functions and $O^\alpha_{\mu_1\mu_2\cdots\mu_n}(0)$ are tensor operators of rank $n$. The scale dimensions of $O^\alpha_{\mu_1\cdots\mu_n}$ determine the behaviors of $E^n_\alpha(z^2)$ near the light cone which in turn determine the behavior of the structure function $W(x, q^2)$ in the Bjorken limit through Eqs. (4) and (1). The violation of strict scaling comes about because the scale dimensions of these operators do not take on their naive canonical values (hence the terminology "anomalous dimensions"). The relevant behavior of $E^n_\alpha(z^2)$ can, in principle, be calculated using the Callan-Symanzik equations.[12] Contact with experiment is established through the moment integrals[13]

$$\int_0^1 dx\, x^n W(x, q^2) = M(n, q^2). \tag{5}$$

The behavior of $M(n, q^2)$ as $q^2\to\infty$ is closely related to the aforementioned singularity behavior of $E^n_\alpha$ [much in the same manner as in Eqs. (2) and (3)]. Thus, typically in CT theories one finds[2,14]

$$M(n, q^2) \to c(n)(q^2)^{-\lambda(n)} \quad \text{as } q^2\to\infty, \tag{6}$$

where $c(n)$ is some unknown constant and $\lambda(n)$ is the (in principle) calculable "anomalous dimension" function associated with the leading tensor operators of Eq. (4).[14] In contrast, the AF theories imply[4,6]

$$M(n, q^2) \to c(n)\left(\ln\frac{q^2}{\mu^2}\right)^{-\lambda(n)} \quad \text{as } q^2\to\infty. \tag{7}$$

In this expression $\mu$ is an unspecified mass scale parameter. The exponent function $\lambda(n)$ is very similar to that in Eq. (6) and can be calculated reliably for any given theory which is asymptotically free. It turns out the functional form of $\lambda(n)$ is rather model independent whereas its normalization depends on the particular gauge group chosen for the theory. We shall discuss the properties of $\lambda(n)$ in both cases [Eqs. (6) and (7)] in some detail later. To pursue the connection with experiment, we assume, for the time being,

$$\lambda(n) = A\tilde{\lambda}(n), \tag{8}$$

where $\tilde{\lambda}(n)$ is a known function of $n$ and $A$ is an undetermined constant.

Equations (6) and (7) are not very useful for practical phenomenological studies because (i) the function $c(n)$ is unknown and (ii) the evaluation of the moment integrals demands experimental information on the structure function at all $x$. Although estimates on $\lambda(n)$ have been made based on Eq. (6) with extrapolated data, the results are not very conclusive.[15] Much more powerful results can be obtained if one assumes[16] the limits in Eqs.

(6) and (7) are reached uniformly in $n$. In that case both of the above-mentioned obstacles can be bypassed and direct predictions on the behavior of the structure function itself can be made provided its initial values at some fixed $q^2 = q_0^2$ are given. One first rewrites Eqs. (6) and (7) in the form

$$M(n, q^2) = M(n, q_0^2) \times \begin{cases} (q^2/q_0^2)^{-\lambda(n)} & \text{(CT)} \\ \left[\dfrac{\ln(q^2/\mu^2)}{\ln(q_0^2/\mu^2)}\right]^{-\lambda(n)} & \text{(AF)}, \end{cases} \tag{9}$$

whereby $c(n)$ is replaced by the function $M(n, q_0^2)$ at fixed $q_0^2$. The two forms of Eq. (9) can be unified and put into a more useful form by a change of variable

$$M(n, k) = M(n, 0) e^{-\tilde{\lambda}(n) k}, \tag{10}$$

where

$$k = \begin{cases} A \ln(q^2/q_0^2) & \text{(CT)} \\ A \ln\left[\dfrac{\ln(q^2/\mu^2)}{\ln(q_0^2/\mu^2)}\right] & \text{(AF)}. \end{cases} \tag{11}$$

Note we have absorbed the unknown constant $A$ [of Eq. (8)] into the definition of $k$ so that Eq. (10) fully determines the function $M(n, k)$ when $\lambda(n)$ is specified (theoretically) and $M(n, 0)$ is given (experimentally). This initial-value problem for the moments $M(n, k)$ can be converted into one for the structure function $W(x, k)$ itself because the defining equation for $M$, Eq. (5), is invertible. In fact, using well-known properties of Mellin (or Laplace) transform[17] one obtains

$$W(x, q^2) = \frac{1}{2\pi i} \int_{\tau - i\infty}^{\tau + i\infty} dn\, x^{-n} M(n, q^2). \tag{12}$$

Hence, substituting (10) into (12) one obtains an equation which determines $W(x, q^2)$ provided $\lambda(n)$ and $W(x, q_0^2)$ are given.[18]

In practice, it turns out, the most convenient way to implement this scheme is to start from the differential form of Eq. (10),

$$\frac{\partial}{\partial k} M(n, k) = -\tilde{\lambda}(n) M(n, k). \tag{13}$$

Then by taking the inverse Mellin transform of this equation, one applies the convolution theorem[18] in evaluating the right-hand side and obtains

$$\frac{\partial}{\partial k} W(x, k) = \int_x^1 dy\, \Lambda(x, y) W(y, k). \tag{14}$$

Here $\Lambda(x, y)$ is related to $\tilde{\lambda}(n)$ by

$$\Lambda(x, y) = -\frac{1}{y} \frac{1}{2\pi i} \int_{\tau - i\infty}^{\tau + i\infty} dn \left(\frac{x}{y}\right)^{-n-1} \tilde{\lambda}(n). \tag{15}$$

Equation (14), together with the initial condition

$$W(x, k = 0) = W(x, q^2 = q_0^2), \tag{16}$$

completely determines the structure function $W(x, q^2)$. Note the integral in (14) only runs from $x$ to 1, i.e., to determine $W(x, q^2)$ we only need to know $W(y, q_0^2)$ for $x < y < 1$. A better way of saying this is the following: *if we know* $W(x, q_0^2)$ *for* $x_0 < x < 1$, *then we can calculate* $W(x, q^2)$ *for any* $q^2$ *with* $x$ *in the same range*. This is important phenomenologically since for fixed $q^2 = q_0^2$, data on $W(x, q_0^2)$ are not available for small $x$ (because of finite incident energy of the accelerators). The predictive power of Eqs. (14)–(16) is illustrated in the kinematic plot, Fig. 1.

The theoretical input necessary for implimenting the above program resides in the function $\lambda(n)$ [or $\tilde{\lambda}(n)$ which differs from it by a constant factor $A$]. Our knowledge on $\lambda(n)$ for various theories is not complete. But some quite general properties as well as a number of specific examples are known. These give us a sufficient handle on $\lambda(n)$ to extract useful predictions on the structure function.

From the fact that the energy-momentum tensor is the dominant second-rank tensor (with isospin zero) and that it must have the canonical scale dimension 4, we know

$$\lambda^s(2) = 0. \tag{17}$$

Here the superscript s stands for "singlet" (or $I = 0$). Moreover, from the fact that $W(x, q^2)$ is the forward virtual Compton amplitude, related to a positive definite total cross section by the optical theorem, it was derived[11] that $\lambda^s(n)$ satisfy the following useful inequalities:

$$\begin{aligned} &\lambda^s(n + m) \geq \lambda^s(n), \\ &\lambda^s(n + m') \leq \lambda^s(n) + \frac{m'}{m}[\lambda^s(n + m) - \lambda^s(n)]. \end{aligned} \tag{18}$$

Here $n, m, m'$ are even positive integers and $m' > m$. A number of interesting consequences im-

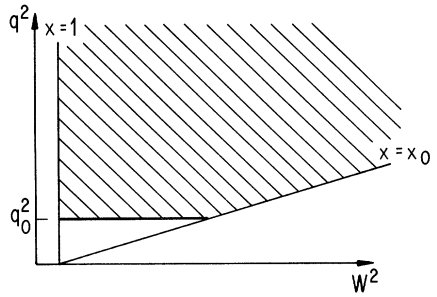


FIG. 1. Kinematic region for deep-inelastic scattering. If the structure functions are given on the heavy line ($q^2 = q_0^2$, $x_0 < x < 1$), their values in the entire hatched region can be calculated from Eq. (14).

mediately follow from these inequalities:

(i) $\lambda^s(n) > 0$ for $n > 2$;

(ii) if $\lambda^s(n_0) = 0$ for any $n_0 \neq 2$, then $\lambda^s(n) = 0$ for all $n$, but this is possible only if the theory is a free field theory;

(iii) $\lambda^s(n)$ can at most increase linearly with $n$.

We mention in advance that these general properties are crucial in giving rise to the pattern of scaling violation to be derived in the next section. For the nonsinglet (ns, or $I \neq 0$) case, the only known general information is

$$\lambda^{ns}(n) \geq \lambda^s(n). \tag{19}$$

As mentioned previously, in any given renormalizable field theory, $\lambda(n)$ are in principle determined by a set of Callan-Symanzik equations.[12] In the case of asymptotically free theories, the coefficient functions in these equations are calculable and $\lambda(n)$ can indeed be determined.[6] We shall return to the explicit form for $\lambda(n)$ in the next section. In the case of conventional-type field theories, these equations can only be solved in certain approximations.[12,13,19] The resulting expressions are consistent with each other and are similar to those obtained for the AF case. In addition, they satisfy the general constraints Eqs. (17) and (18). We can, therefore, use these expressions with some confidence. Possible effects due to the remaining uncertainties can be investigated phenomenologically by adopting certain general parametrization of $\lambda(n)$ consistent with the constraints (17) and (18) and studying the dependence of the predictions on the parameters.

We already mentioned that the normalization constant $A$ for $\lambda(n)$ is determined by the structure of the gauge group in the case of AF theories. Insofar as there are many possible candidates for this group, the value of $A$ is somewhat constrained but not determined by theory. In the case of CT theories, one has very little handle on $A$. It is related either to the coupling constant in perturbation calculations[12,13] or to the $\epsilon$ parameter in the $(4-\epsilon)$-dimension calculation.[19] It appears, therefore, that the most prudent approach is to leave $A$ as an unknown parameter to be determined by experiment.

## III. APPLICATION TO ELECTROPRODUCTION

The formalism of the previous section can be applied to the realistic case of electroproduction in a straightforward manner. We now have two independent structure functions $W_1$ and $\nu W_2$. The relevant moment integrals are

$$\begin{aligned} &\int_0^1 dx\, x^{n-1} W_1(x, q^2) = M_1(n, q^2), \\ &\int_0^1 dx\, x^{n-2} \nu W_2(x, q^2) = M_2(n, q^2). \end{aligned} \tag{20}$$

Here again the large-$q^2$ behavior of $M_i(n, q^2)$ is expected to be of the form represented by Eq. (10). Carrying through the program outlined in Sec. II, one can again calculate $W_i(x, q^2)$ for all $(x, q^2)$ provided theory supplies $\lambda(n)$ and experiment supplies $W_i(x, q_0^2)$ at some $q_0^2$. In the following, we shall only explicitly deal with $\nu W_2$ which we simply write as $F$, i.e.,

$$F(x, q^2) = \nu W_2(x, q^2). \tag{21}$$

The corresponding formulas for $W_1$ can be obtained by replacing $xW_1$ for $F(x, q^2)$ in all subsequent formulas.

The required experimental input, $F(x, q^2)$ for fixed $q_0^2$, exists at present only for proton target. For this reason, we shall restrict ourselves to this case. The initial value $q_0^2$ is chosen to be $q_0^2 = 4$ GeV since this is a reasonably large $q^2$ at which data over an extended range in $x$ exist. Throughout this paper we shall take "large $q^2$" to mean $q^2 > 4$ GeV$^2$. This is certainly within the deep-inelastic region where the structure functions are observed to vary only slowly with $q^2$ for fixed $x$. Consequently, the asymptotic equations of the previous section should apply. (Theory itself does not say what $q^2$ is asymptotic.) Needless to say, entirely similar calculations can be carried out with other initial conditions appropriate for other targets.

The required theoretical input function $\tilde{\lambda}(n)$ satisfies the same general requirements as discussed in the previous section for the scalar current case. The specific form for $\tilde{\lambda}(n)$ can be calculated more readily for the asymptotically free theories. It was shown that the situation is simplest for the isospin nonsinglet (ns) case where

$$\tilde{\lambda}^{ns}(n) = -3 - 2/n(n+1) + 4\sum_{m=1}^{n} (1/m). \tag{22}$$

However, we are more interested in the isospin singlet (s) piece which dominates the proton structure functions at large $q^2$ [cf. Eqs. (10) and (19)]. The situation is slightly more complicated here because for each $n$, several tensor operators play a role. We do not have a simple closed formula like Eq. (22). Fortunately, we already know $\lambda^s(2) = 0$ and $\lambda^s(n+1) > \lambda^s(n)$ from general grounds (Sec. II). The additional knowledge[20] that $\lambda^{ns}(n) - \lambda^s(n)$ is very small for all except $n = 2$ (i.e., $n > 4$) then severely restricts the possible behavior of $\lambda^s(n)$. The results previously reported in Ref. 7 and reproduced in the following are calculated with the phenomenological formula

$$\tilde{\lambda}^s(n) = -3 - 18/n(n+1) + 4\sum_{m=1}^{n} (1/m) \tag{23}$$

which satisfies the above requirements. Other possible forms have also been studied and found to yield qualitatively similar results. These will be discussed in Sec. VI.

For conventional field theories, $\tilde{\lambda}(n)$ cannot be obtained without using approximation methods. Several basically different approaches yield very similar results which in addition are consistent with the general constraints of Sec. II. A typical form is

$$\tilde{\lambda}^s(n) = 1 - 6/n(n+1). \tag{24}$$

This expression is similar to the first two terms of the corresponding formula for the asymptotically free case, Eqs. (22) and (23). It is obtained both from perturbation calculation of the Callan-Symanzik coefficient functions[12] and from Wilson's $(4-\epsilon)$-dimension method.[19] Other more elaborate approximation methods lead to results milder than (24) in the sense that the poles at $n=0$ and $-1$ are either softened to a cut[19] or moved farther from the physical values[13] ($n>2$) resulting in milder apparent scaling violation for the same value of $A$ (the normalization constant relating $\lambda$ to $\tilde{\lambda}$). Since this constant is not known *a priori*, very similar patterns of scaling violation are obtained from the various formulas when the scale is set by an experimental input point. For this reason, we shall use the simplest and most singular case, Eq. (24), as an explicit example in the following discussions. Sensitivity of the results to the other possible choices of $\lambda^s$ will be explored in Sec. VI.

Carrying through the program outlined in the previous section with the input $\tilde{\lambda}(n)$ of Eq. (23) for the AF case, we obtain the following equations for the structure function

$$\begin{aligned} &k = A \ln\left[\frac{\ln(q^2/\mu^2)}{\ln(q_0^2/\mu^2)}\right], \\ &F(x, k=0) = F(x, q^2 = q_0^2), \\ &\frac{\partial}{\partial k}F(x,k) = [3 + 4\ln(1-x)]F(x,k) + \int_x^1 dy \frac{x}{y^2}\left[18\left(1-\frac{x}{y}\right)F(y,k) + 4\frac{(x/y)F(y,k) - F(x,k)}{1-(x/y)}\right]. \end{aligned} \tag{25}$$

Likewise, with the simpler formula, Eq. (24), for the CT case, we obtain

$$\begin{aligned} &k = A\ln(q^2/q_0^2), \\ &F(x, k=0) = F(x, q^2 = q_0^2), \\ &\frac{\partial}{\partial k}F(x,k) = -F(x,k) + 6\int_x^1 dy \frac{x}{y^2}\left(1-\frac{x}{y}\right)F(y,k). \end{aligned} \tag{26}$$

Given $F(x, k=0)$ for $0<x<x_0$, these equations can be trivially integrated numerically to yield $F(x,k)$ for all $k$ and $0<x<x_0$.

The results of such a calculation are presented in Figs. 2–5. In Fig. 2 and Fig. 3 we give the familiar plot of the structure function vs the variable $x$ for some fixed values of $k$ ($\sim q^2$). One sees the well-known trend of an increasingly peaked curve $F(x, q^2)$ toward small $x$ as $q^2$ increases for both the AF (Fig. 2) and the CT (Fig. 3) case. The area under the curve remains constant in all cases. To see the scaling violation effects more vividly, it is more convenient to plot the structure function vs $k$ ($\sim q^2$) for fixed values of $x$. This is done in Fig. 4 and Fig. 5 for the AF and CT cases, respectively. If strict Bjorken scaling holds, $F(x, q^2)$ would be independent of $q^2$ and all the curves in these plots would be horizontally flat. The predicted curves show $F(x, q^2)$ as an increasing function of $q^2$ for small $x$ and a decreasing function of

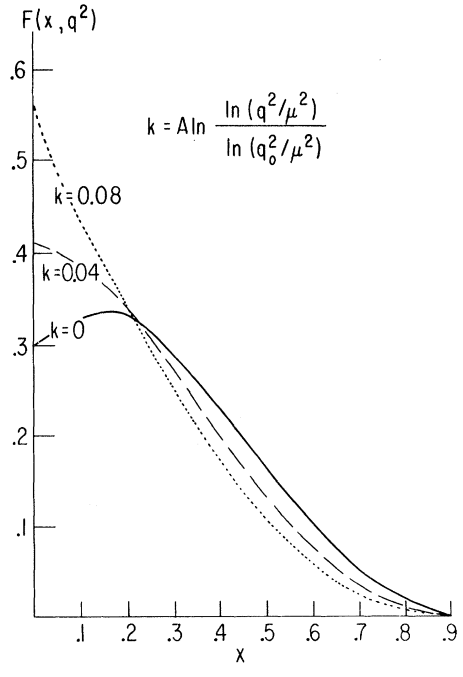


FIG. 2. The structure function $F(x, q^2)$ plotted against $x$ for three values of $k$ in the AF model, Eq. (23). The $k=0$ curve is the experimental input $F(x, q^2 = 4\ \text{GeV}^2)$.

$q^2$ for larger $x$.

This pattern of scaling violation is qualitatively different from that implied by most phenomenological scaling violating models.[8] These models predict structure functions which have factorized dependences on $x$ and $q^2$, i.e., $W_i(x, q^2) = G_i(q^2) F_i(x)$, for large $q^2$. This means the dependence on $q^2$ would be independent of $x$ except for normalization. In terms of a plot like Fig. 4 (or 5), the curves for different $x$ would then all be parallel. The distinction between the two cases will be very marked.

## IV. DISCUSSION OF GENERAL RESULTS

The first impression one obtains by glancing at Figs. 2–5 is the apparent similarities between the predictions of conventional and asymptotically free theories. The only differences lie in the scale of the variable $k$ and the different relations of this quantity to the physical variable $q^2$, Eq. (11). We will discuss first the common features, their physical origins, and then the differences and their significance.

The broad trends observed in the last section are previously known and are attributable to the general properties of the theoretical framework previously discussed. From Eq. (20) we see that the $n=2$ moment of $F(x, q^2)$ (in the variable $x$) is

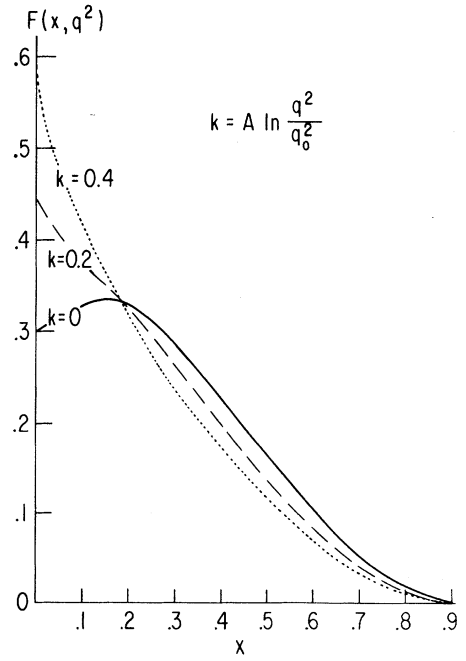


FIG. 3. The structure function $F(x, q^2)$ plotted against $x$ for three values of $k$ in the CT model, Eq. (24). The $k=0$ curve is the experimental input $F(x, q^2 = 4\ \mathrm{GeV}^2)$.

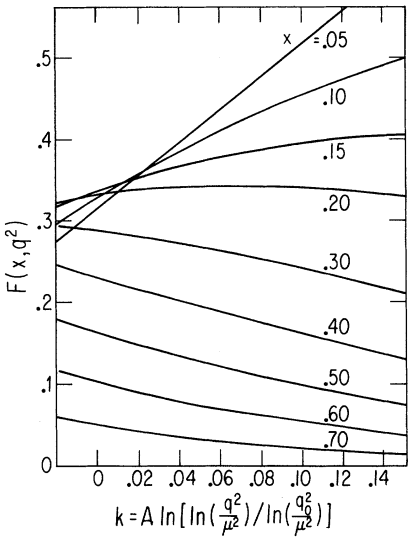


FIG. 4. The structure function $F(x,k)$ calculated from the AF model, Eq. (24), plotted against $k$ for fixed values of $x$.

equal to the area under the curves in Figs. 2 and 3. The fact that this area remains constant for different values of $q^2$ is a direct consequence of the general requirement $\lambda^5(2) = 0$, Eq. (17). In contrast, the higher moments do depend on $q^2$. They are all decreasing functions of $q^2$ because $\lambda(n) > 0$ when $n > 2$ [cf. Eqs. (6) and (7) and the discussion following Eqs. (18) and (19)]. As the higher moments of $F(x, q^2)$ are more sensitive to its value

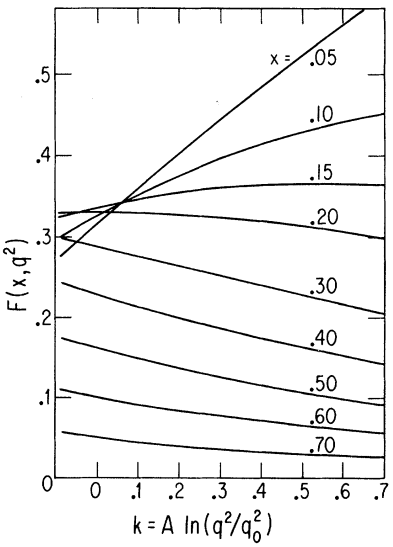


FIG. 5. The structure function $F(x,k)$ calculated from the CT model, Eq. (24), plotted against $k$ for fixed values of $x$.

near $x=1$, $F(x, q^2)$ must be a decreasing function of $q^2$ for large $x$ (i.e., near $x=1$). The conservation of area under the $F(x, q^2)$ curve then implies the opposite behavior, i.e., that $F(x, q^2)$ be an increasing function of $q^2$, at the lower end of the $x$ range ($x \sim 0$). This is, of course, just the pattern we observed from our explicit calculations.

It is to be noted that for any fixed $x$, $F(x, q^2)$ eventually decreases to zero provided one goes to sufficiently large $q^2$ [the only exception being $x=0$ where $F(0, q^2)$ increases indefinitely with $q^2$]. On the other hand, for any fixed range of $q^2$ (accessible to experiment), there are always three different regions of the $x$ variable within which $F(x, q^2)$ has distinct dependences on $q^2$: increasing, decreasing, and approximately constant. Our calculations, of which the cited examples are typical cases, reveal that one can go beyond this general observation. In fact, within the range of $q^2$ covered by foreseeable experiments, we found a number of specific features of this pattern of scaling violation which are universally shared by the different types of theories and are quite independent of the theoretical uncertainties associated with the calculational scheme. We state these features here (cf. Fig. 4 and Fig. 5):

(1a) For $0.25 < x < 1$, $F(x, q^2)$ is a decreasing function of $q^2$,

(1b) the rate of decrease in $q^2$ is greatest for $x \simeq 0.4$ and tapers off at both ends;

(2) In the vicinity of $x \simeq 0.2$, $F(x, q^2)$ has little or no dependence on $q^2$—this is the "apparent" scaling region;

(3a) For $0 < x < 0.15$, $F(x, q^2)$ is an increasing function of $q^2$,

(3b) the rate of increase grow monotonically as $x$ approaches zero. This universal pattern holds to within 0.05 in the values of $x$ quoted for the wide range of theoretical models that we have explored (cf. Sec. VI).

Why is this pattern of scaling violation so specific for such a wide class of theories? We have already discussed the origin of the qualitative pattern [namely, $\lambda(2)=0$ and $\lambda(n) > \lambda(n-1) > 0$]. In addition, the fact that the transition from an increasing to decreasing dependence of $q^2$ occurs closer to the lower end of $x$ ($\sim 0.2$) follows, to a large extent, from the shape of the input experimental curve $F(x, q_0^2)$. It is not hard to see from Eqs. (25) and (26) that since $F(x, q_0^2)$ is tilted toward the lower end, the rate of change of $F(x, k)$ in $k$ is also greater in this region. The conservation of area then implies that the crossing point be nearer to the lower end in $x$.

To shift from the general pattern to the details we need to discuss the scale of the variable $k$ and its precise relation to $q^2$. In particular, in order to compare the specific results of Figs. 4 and 5 with each other and with experiment, we need to fix the hitherto unspecified parameters $A$ and $\mu$ [cf. Eqs. (25) and (26)]. We have explained (cf. Sec. II) that these parameters are model dependent and should be determined by experiment. All that is needed is to pick one (or two) well-measured points for $F(x, q^2)$ at fairly large $q^2$ and compare with the theoretical curves; that will determine the constant $A$ (and, for the AF case, also $\mu$). This will be done in the next section.

Before turning to that, let us briefly comment on the anticipated qualitative difference between the two types of theories, AF vs CT, as exemplified by the two special cases shown by Figs. 4 and 5. To compare, we have to plot the results on the same scale. Let us imagine converting the horizontal log-log $q^2$ scale of Fig. 4 into the log $q^2$ scale as in Fig. 5. What would the effects on the curves be? Obviously, the general trends for the curves will remain the same except the variation of the curves will be compacted near the lower $q^2$ end and stretched in the higher $q^2$ range. Since the apparent shape of the curves in Figs. 4 and 5 started out very similarly, we anticipate detectable differences between the predictions of these two types of theories only at low (near $q_0^2$) and very high (asymptotic) $q^2$.

## V. COMPARISON WITH DATA

Shown in Figs. 6 and 7 are data on $F(x, q^2)$ from SLAC[9] plotted against $q^2$ for several values of $x$. The range of $q^2$ covered is fairly large for $0.4 < x < 1$, but becomes very restricted toward the lower

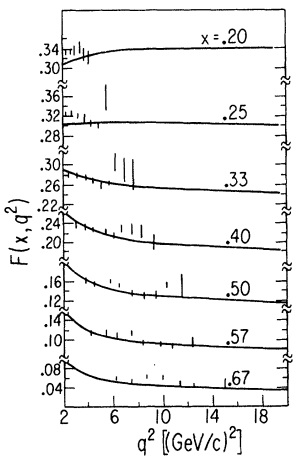


FIG. 6. The structure function $F(x, q^2)$ plotted against $q^2$. The curves are calculated from the AF model, Eq. (23), with $A=0.085$, $\mu=1$ GeV. The data points are from Ref. 9.

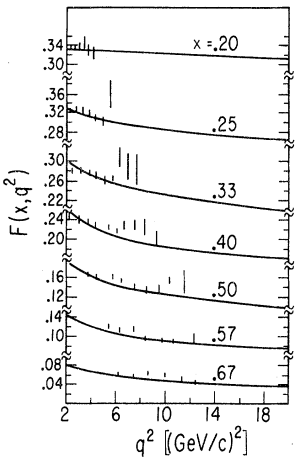


FIG. 7. The structure function $F(x, q^2)$ plotted against $q^2$. The data points are from Ref. 9. The curves are calculated from the CT model, Eq. (24), with $A = 0.25$.

end of $x$. The main feature of approximate scaling holds to within 20–30% over the measured ranges of $q^2$. We are, of course, interested in the deviation from strict scaling. In this respect one discerns a systematic decrease of $F(x, q^2)$ as a function of $q^2$ in the measured range of $x$. To compare this pattern of deviation from scaling with the theoretical calculations, we use one of the measured points [at $x = 0.57$, $q^2 = 10$ (GeV/$c$)$^2$] to determine the unknown scale parameter $A$ and, for the AF case, choose a "reasonable value" 1 GeV for $\mu$.[20] The predicted curves of $F(x, q^2)$ for the same $x$ values (as the measured ones) are then plotted on Figs. 6 and 7 for the AF and CT cases, respectively. The value of $A$ turns out to be 0.085 for the AF theory and 0.25 for the CT case.

We now make a series of remarks on the comparison between theory and data.

(i) The observed general trend of $F(x, q^2)$ falling with $q^2$ in the range $0.25 < x < 1$ is certainly in accord with the theoretical expectation as stated in point (1a) of Sec. IV.

(ii) The rate of decrease with $q^2$ within the range seems to be in general agreement with the predictions of both types of theories also [(1b) of Sec. IV]. It is to be noted, however, this agreement is not really so striking since (i) the range of $q^2$ is limited on the lower $x$ end, and (ii) the experimental input point was chosen near the upper $x$ end.

A new experiment at SLAC[21] is expected to measure the structure functions in the same $x$ range but extending to larger values of $q^2$. With the addition of these new data we hope a more meaningful test of the predictions can be made.

(iii) The value of $A \sim 0.085$ obtained for the AF case is compatible with typical theoretical values like $\frac{4}{27}$ for some popular choice of the gauge group[6]; the value $A = 0.25$ for the CT case does not have any unique theoretical interpretation; it is consistent with previous crude estimates of the same parameter.[15,18]

(iv) Crucial tests of the theoretical ideas can, in principle, be furnished by data at low values of $x$, as theory predicts quite different $q^2$ dependence in this region. For the present, however, useful data of this type do not yet exist. (As seen from Figs. 6 and 7, even for $x = 0.2$ we have no data beyond $q^2 = 4$.) Fortunately, this is exactly the kinematic region where most data from the new generation of $\mu N$ deep-inelastic scattering experiments at very high energies are expected to lie.[10] The new data should provide us with a good test of the predicted pattern [points (2), (3a), and (3b), Sec. IV] and hence the underlying theoretical principles.

There are, of course, already some preliminary data on deep-inelastic $\mu N$ scattering available from Fermilab.[10] However, this very first experiment is not designed to provide the detailed information necessary for a direct comparison with our previous analysis. We shall, therefore, restrict ourselves to a few qualitative remarks. As is the case with the first SLAC-MIT experiment, the most prominent feature of the new data over greatly expanded kinematic ranges is the approximate scaling behavior of the structure functions. However, we are, of course, interested in the finer deviations from strict scaling.

The preliminary data do seem to show a systematic, dependence of the ratio of cross sections at different energies on the (scaled) variable $q^2$. In particular, there seem to be many more events for low $q^2$ (scaled) at high energies than at low energies. At this stage, events are not separated into $x$ bins (as is needed for a more direct comparison with our discussions).[21a] However, because of kinematic constraints, the low $q^2$ events are predominantly associated with small $x$. Inasmuch as we expect the structure functions to be an increasing function of $q^2$ at small $x$, this trend agrees with theoretical predictions. At larger values of $q^2$, the events involve larger values of $x$. The preliminary data indicate a possible falloff with increasing $q^2$, again in agreement with the theoretical pattern, but this is not yet well established.[21a] Clearly, to obtain a more definitive comparison, one has to wait for the more refined data from this as well as other deep-inelastic scattering experiments at the high-energy accelerators. We note in passing that the range of $x$ values covered in the new generation of experiments at Fermilab is roughly[10] $0 < x < 0.4$, thus nicely complimenting the existing ranges measured at lower

energies.

Our comparison of the predicted pattern of scaling violation with existing data, although not conclusive, indicates the potential for shedding light on the theoretical issues and helps to put certain crucial features in focus for the interpretation of new experimental results. In this connection it is perhaps worthwhile emphasizing the importance of looking at the $q^2$ dependence of the measured quantities *separately* in the three regions $x<0.15$, $x\simeq 0.2$, and $x>0.25$. Interesting distinctive features in these regions can be easily washed out in any averaging procedure. In a different vein, even in a crude experiment where the structure functions are not directly measured, one can go beyond the very qualitative comparison of theory and experiment as discussed above. The specific pattern of scaling violation stated previously can be tested by feeding the theoretical predictions into the Monte Carlo calculations made in comparing high-energy and low-energy data.

At the end of Sec. III we mentioned the difference in the patterns of scaling violation implied by field theory and those by phenomenological (parton) models. What can we say about this point in the light of these available data? Within the range of the SLAC data, we cannot tell the difference. However, the two points of view imply opposite $q^2$ dependences for the structure functions at small $x$. In particular, the feature of factorized $x$ and $q^2$ dependences for the phenomenological models implies the structure functions should decrease in $q^2$ at small $x$ (since they are found to do so at large $x$). As already pointed out, the initial indications from the $\mu$-$N$ experiments at Fermilab are that the opposite is true. Thus, if this result holds up, the pattern of scaling violation implied by these phenomenological models can be ruled out whereas that implied by field theory will prove worth further scrutiny.

## VI. DISCUSSION OF THEORETICAL UNCERTAINTIES AND COMPARISON OF AF AND CT THEORIES

So far we have not discussed the theoretically important issue of differentiating the AF and CT theories by comparing their predicted scaling violation effects against each other. (By seeing whether the differences are experimentally distinguishable, one can evaluate the prospect for deciding which type of theory is more likely to be relevant for strong interaction physics.) To carry out this comparison, we have to know the theoretical uncertainties associated with the predictions. (The "typical examples" cited in the previous sections do not give information on this question.) The uncertainties obviously have mainly to do with the CT theories where no demonstrably valid approximation scheme is at our disposal. We attack this problem by a phenomenological approach. Based on the fairly restrictive general constraints, Eqs. (17) and (18), and the specific examples of $\lambda(n)$ given by the various models, we adopt the following parametrization for the effective exponent function

$$\tilde{\lambda}(n)=-\frac{\beta}{(n+\alpha)(n+\alpha+1)}-\gamma+\delta\sum_{m=1}^{n}\frac{1}{m} \tag{27}$$

subjected to the conditions

$$\tilde{\lambda}(2)=0,\qquad \frac{d}{dn}\tilde{\lambda}(n)>0. \tag{28}$$

Here $\alpha$ controls the location of the pole in the pole term (in $n$), whereas $\beta$, $\gamma$, and $\delta$ controls the relative magnitudes of the *pole*, the *constant*, and the *logarithm*[22] terms, respectively. We then calculate the predicted structure function $F(x,k)$ based on this $\tilde{\lambda}(n)$ for a variety of values of the parameters and compare the results within the experimentally accessible region of $q^2$. Features of the predicted structure function (both qualitative and quanitiative) which are generally independent of the parameters are interpreted as consequences of the rigorously established constraints and hence model independent. (These are the results quoted in Sec. IV.) The range of variations of the predictions obtained for different sets of parameters is taken to give an estimate of the theoretical uncertainty associated with this approach. Several examples of these trial calculations are given in Fig. 8. These graphs should also be compared with Figs. 2 and 3.

It is perhaps worth pointing out that the reasons we can extract a set of fairly specific features of scaling violation effects in spite of the theoretical uncertainties represented by Eq. (27) are the following.

(i) Within the available range of $q^2$, many asymptotically different patterns are indistinguishable.

(ii) As the overall constant $A$ is adjusted to fit with experiment, often the effects due to different choices of the parameters $\alpha, \beta, \gamma, \delta$, can be absorbed by a change of $A$.

Beyond the features cited in Sec. IV, it is very hard to distinguish more quantitative differences between specific models. The reasons, separately mentioned before, are the following: (i) we only used a one-term (effective) formula in the high-energy expansion [cf. Eq. (10)], (ii) there is always the ambiguity associated with which "scaling variable" to use,[23] (iii) the uncertainty associated with

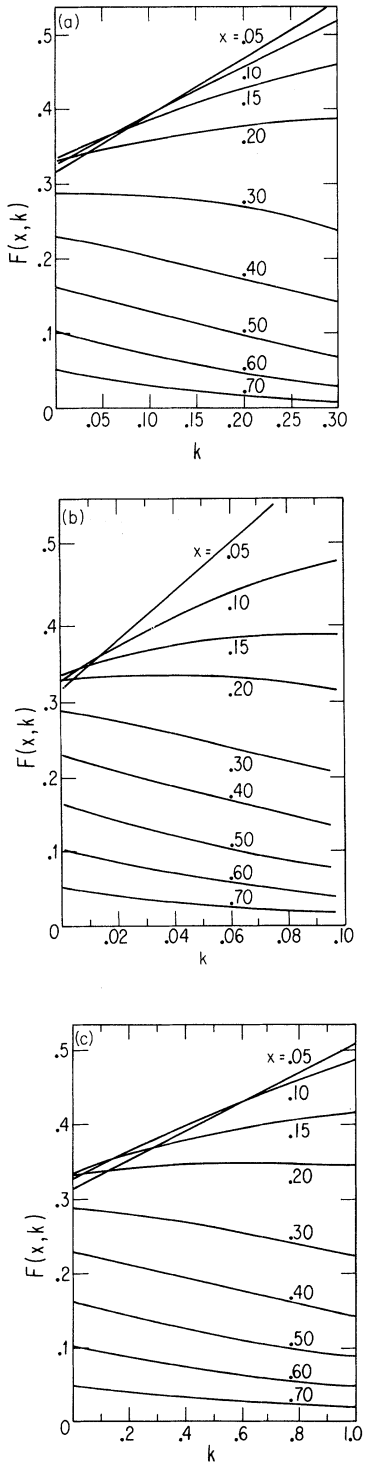


FIG. 8. Calculated $F(x,k)$ from typical extreme cases of the phenomenological formula, Eq. (27): (a) $\beta=0$, $\gamma=6$, $\delta=4$; (b) $\alpha=0$, $\beta=36$, $\gamma=0$, $\delta=4$; (c) $\alpha=2$, $\beta=20$, $\gamma=-1$, $\delta=0$. The examples given previously correspond to $\alpha=0$, $\beta=18$, $\gamma=3$, $\delta=4$ (Fig. 2) and $\alpha=0$, $\beta=6$, $\gamma=-1$, $\delta=0$ (Fig. 3).

the precise form of $\lambda(n)$ in CT theories, and (iv) we do not know what the parameter $\mu$ is for AF theories. There is, of course, one significant difference between AF and CT theories—they predict different asymptotic $q^2$ dependence for the structure functions. In our calculations, this difference manifests itself in the different relations between the (physical) variable $q^2$ and the variable $k$ (which is conveniently chosen for calculations), Eq. (11). However, within the experimentally accessible $q^2$ range, this difference is insignificant as compared to the other uncertainties inherent in each class of theories by themselves.

In conclusion, then, we see the deep-inelastic scattering as offering an excellent test of the general features of scaling violation implied by field theory. These features are in accord with the trends of available preliminary data and will be crucially tested in the very near future. A combination of theoretical uncertainties and experimental limitations prevents the possibility of distinguishing the predictions of AF vs CT field theories. The choice with regard to which of these theories is more likely to be the one underlying strong-interaction dynamics will remain a matter of aesthetic appeal until a better test is devised.

## ADDENDUM

Since this paper was written, more definitive results from the first Fermilab $\mu$-$N$ inelastic scattering experiment have become available[24, 25] Extensive data obtained at 56 GeV/$c$ and 150 GeV/$c$ incoming muon energies are compared with each other (Ref. 24) as well as with calculated extrapolations from the much lower energy SLAC data assuming strict scaling (Ref. 25). These comparisons, especially the second one, show a clear pattern of scaling noninvariance in the measured kinematic region (which spans a $q^2$ range of 5 $(\mathrm{GeV}/c)^2$ at $x\simeq 0.03$ increasing to 30 $(\mathrm{GeV}/c)^2$ at $x\simeq 0.3$). Although this experiment does not measure the structure function $\nu W_2(x, q^2)$ directly, information on the $(x, q^2)$ dependences has been extracted from Monte Carlo calculations. The systematic change of the $q^2$ dependence as a function of $x$ agrees very well with the pattern predicted from our field theory calculations (Sec. IV). Thus $\nu W_2$ is a decreasing function of $q^2$ in the range $0.2<x<0.3$, it remains fairly constant at $x\simeq 0.2$ and becomes an increasing function of $q^2$ for $x<0.2$. The rate of change of $\nu W_2$ as a function of $q^2$ was found to increase monotonically as $x$ decreases from $x\simeq 0.3$ to $x\simeq 0.03$. This is again in accord with our prediction. Theory predicts this rate of change will have a minimum (negative maximum) at $x\simeq 0.4$ and increase to zero as $x$ in-

creases from $x=0.4$ to 1. This latter behavior is already confirmed by the SLAC results as treated in the text.

The observed pattern of scaling noninvariance clearly disagrees with that expected from modified parton models.[8] As discussed in the text, these models imply similar $q^2$ dependence for all ranges of $x$.

The rise in $\nu W_2$ with $q^2$ at small $x$ can be attributed to the excitation of new degrees of freedom.[26] This point of view is not very quantitative; it also only applies to the large $\omega$, or diffractive, region. It is, however, not incompatible with the field theoretical considerations discussed in this paper. In fact, if one accepts the rise with $q^2$ at small $x$ (as due to the excitation of new degrees of freedom) and also the constancy of the area under the $\nu W_2$ curve (as due to the dominance of the energy-momentum tensor in the second moment integral) then one arrives at an alternative "explanation" of why the structure function falls with $q^2$ at large $x$.

---

*Work supported in part by the National Science Foundation under Contract No. MPS74-08833.

†Present address: Illinois Institute of Technology, Chicago, Ill. 60616.

[1]R. P. Feynman, *Lepton-Hadron Scattering* (Benjamin, Reading, Mass., 1972).

[2]For useful reviews and extensive references see K. Wilson, in *Proceedings of the 1971 International Symposium on Electron and Photon Interactions at High Energies*, edited by N. Mistry (Cornell Univ. Press, Ithaca, 1972), and Y. Frishman, Phys. Rep. 13C, 1 (1974).

[3]G. Parisi, Phys. Lett. 42B, 114 (1972); C. Callan and D. Gross, Phys. Rev. D 8, 4383 (1973).

[4]D. J. Gross and F. Wilczek, Phys. Rev. Lett. 30, 1343 (1973); H. D. Politzer, *ibid.* 30, 1346 (1973).

[5]By "conventional" we mean renormalizable field theories which are not asymptotically free or, alternatively, theories which have fixed points at finite but nonzero values.

[6]G. Parisi, Phys. Lett. 50B, 367 (1974); H. Georgi and H. D. Politzer, Phys. Rev. D 9, 416 (1974); D. Gross and F. Wilczek, *ibid.* 9, 980 (1974); D. Gross, Phys. Rev. Lett. 32, 1071 (1974); A. De Rújula *et al.*, Phys. Rev. D 10, 2141 (1974); A. Zee *et al.*, *ibid.* 10, 2881 (1974).

[7]A brief account of the results of this study has been given by Wu-ki Tung, Phys. Rev. Lett. 35, 490 (1975).

[8]M. Chanowitz and S. Drell, Phys. Rev. Lett. 30, 807 (1973); V. Barger, Phys. Lett. 49B, 43 (1974); G. West and P. Zerwas, Phys. Rev. D 10, 2130 (1974).

[9]G. Miller *et al.*, Phys. Rev. D 5, 528 (1972); A. Bodek *et al.*, Phys. Lett. 52B, 259 (1974) and references cited therein.

[10]D. J. Fox *et al.*, Phys. Rev. Lett. 33, 1504 (1974).

[11]O. Nachtmann, Nucl. Phys. B63, 237 (1973).

[12]N. Christ, B. Hasslacher, and A. Mueller, Phys. Rev. D 6, 3543 (1972).

[13]G. Mack, Nucl. Phys. B35, 592 (1971); in *Strong Interaction Physics, Lecture Notes in Physics*, edited by W. Ruehl and A. Vancura (Springer, Berlin, 1972), Vol. 17.

[14]This simple form is based on the assumption that one tensor operator of each rank $n$ dominates at large $q^2$. In general, when several operators contribute, a sum of several terms should be included. For the qualitative features of scaling violation that we shall be concerned with, however, the simple form, Eq. (6), suffices. $\lambda(n)$ can be regarded as an "effective" anomalous dimension much in the same spirit as "effective Regge trajectory" is used in the description of high-energy behavior of two-body scattering amplitudes.

[15]E. Bloom, *Proceedings of the Sixth International Symposium on Electron and Photon Interactions at High Energy, Bonn, Germany, 1973*, edited by H. Rollnik and W. Pfeil (North-Holland, Amsterdam, 1974). S. I. Bilenkaya *et al.*, Nucl. Phys. 79B, 422 (1974); O. Nachtman, *ibid.* 78B, 455 (1974).

[16]This assumption is not justified on theoretical grounds.

[17]See P. M. Morse and H. Feshbach, *Methods of Theoretical Physics* (McGraw-Hill, New York, 1953), Vol. 1, pp. 467–471.

[18]This technique for evaluating the structure function was proposed by G. Parisi, Phys. Lett. 43B, 107 (1973); 50B, 367 (1974).

[19]K. Wilson, Phys. Rev. D 8, 2911 (1973); C. Lovelace, Rutgers report, 1974 (unpublished).

[20]One could also use a second experimental point as input to determine $A$ and $\mu$ simultaneously. The results would be similar.

[21]W. B. Atwood *et al.*, given at XVII International Conference on High Energy Physics, London, 1974 (referred to in reports) and SLAC Red Report No. 185 (unpublished).

[21a]Note added in proof. See the Addendum for recent developments on this point.

[22]$\Sigma_{m=1}^{n}(1/m)$ behaves like $\ln n$ for large $n$.

[23]We used $x=q^2/2M\nu$. There are many other possible choices, among which $x'=q^2/(2M\nu+M^2)$. The difference between two choices manifests itself in the second leading term in the high-energy expansion. In this sense, point (ii) is related to point (i). Our approach is to adhere to one choice of the scaling variable, treat data expressed in that variable, and regard the one-term expansion formula as an effective representation. The resulting phenomenology will then be largely independent of the choice of the scaling variable.

[24]Y. Watanabe *et al.*, Phys. Rev. Lett. 35, 898 (1975).

[25]C. Chang *et al.*, Phys. Rev. Lett. 35, 901 (1975).

[26]H. T. Nieh, Phys. Lett. 53B, 344 (1974); D. Schildknecht and F. Steiner, Phys. Lett. 56B, 36 (1975); F. Hayot and H. T. Nieh, Phys. Rev. D 12, 2907 (1975).